



Magnetic relaxation in the vicinity of second magnetization peak in BSCCO crystals

M. Konczykowski^{a,*}, S. Colson^a, C.J. van der Beek^a, M.V. Indenbom^{a,b},
P.H. Kes^c, E. Zeldov^d

^a *Laboratoire des Solides Irradiés, Ecole Polytechnique, CNRS URA-1380, 91128 Palaiseau, France*

^b *Institute of Solid State Physics, 142432 Chernogolovka, Russia*

^c *Kamerlingh Onnes Laboratorium, Rijksuniversiteit Leiden, 2300 RA Leiden, The Netherlands*

^d *Department of Condensed Matter Physics, Weizmann Institute of Science, Rehovot, Israel*

Abstract

We have used Hall array and magneto-optic techniques for the investigation of magnetic relaxation in clean $\text{Bi}_2\text{Sr}_2\text{CaCu}_2\text{O}_8$ (BSCCO) crystals. The enhancement of the bulk critical current seen as a second peak in the magnetization curves is identified with the discontinuous change of the flux creep energy barrier vs. current relation. We propose a consistent interpretation of the hysteretic magnetization and its relaxation in clean BSCCO crystals, based on the presence of two distinct vortex matter phases, manifesting different electrodynamics. Special attention will be given to the motion of the interface between those phases across the sample. © 2000 Published by Elsevier Science B.V. All rights reserved.

Keywords: Magnetic relaxation; Second magnetization peak; BSCCO; Vortex matter phases

1. Introduction

Most of the high-temperature superconductors exhibit a magnetic field-induced enhancement of the irreversible magnetization called “second magnetization peak” (SP). The investigation of the effect of controlled disorder on both the SP (observed in the irreversible magnetization at temperatures below 35 K) and the closely related jump in the reversible magnetization (identifying the first order transition above 35 K) in highly anisotropic $\text{Bi}_2\text{Sr}_2\text{CaCu}_2\text{O}_8$ (BSCCO) has led to the general acceptance of a phenomenological phase diagram of the vortex lattice containing three distinct phases: the vortex liq-

uid, the crystalline and glassy solid phases [1–5]. A theoretical background for such a diagram was given by several models predicting a solid–solid phase transition from a quasi-ordered low magnetic field phase to a disordered high field phase [6–8]. The suggestion that this scenario can be applied to other superconductors including cubic $(\text{K}_x\text{Ba}_{1-x})\text{BiO}_3$ is supported by neutron diffraction and muon spin rotation experiments, which identify a structural transformation of vortex matter at the SP field [9–11]. Magnetic relaxation experiments in the vicinity of the SP have attracted a lot of attention because they can provide insight into the electrodynamics of the two solid phases and the mechanism of the phase transition. Unfortunately, conventional global magnetization measurements which account for most

* Corresponding author.

published work have two limitations: the surface barrier and bulk pinning contributions are difficult to distinguish, and the hypothetical phase transition driven by the local value of the magnetic induction is hard to follow. By using local measurements by Hall probe arrays and magneto-optics, we avoided those problems and we explored the energy barrier vs. current relations in the vortex phases below and above the SP.

2. Experiment

The experiments were carried out on BSCCO crystals grown by the travelling solvent floating zone

technique. Rectangles of typical dimensions 0.3×0.7 mm² were cut from a bigger crystal after imaging of the flux penetration by magneto-optics and elimination of the defective regions. The Hall array composed of 11 sensors of area 10×10 μm² each separated by 10 μm was centered on top of the crystal, parallel to the short axis of the rectangle. All experiments were carried out with the DC magnetic field, H_a , applied perpendicular to the surface (parallel to the c -axis of the crystal).

Typical examples of hysteresis loops recorded at temperatures below 35K are shown in Fig. 1. The local magnetization, $H_s = B_{loc} - H_a$ defined as the difference between the magnetic induction measured at a probe location and the applied magnetic field,

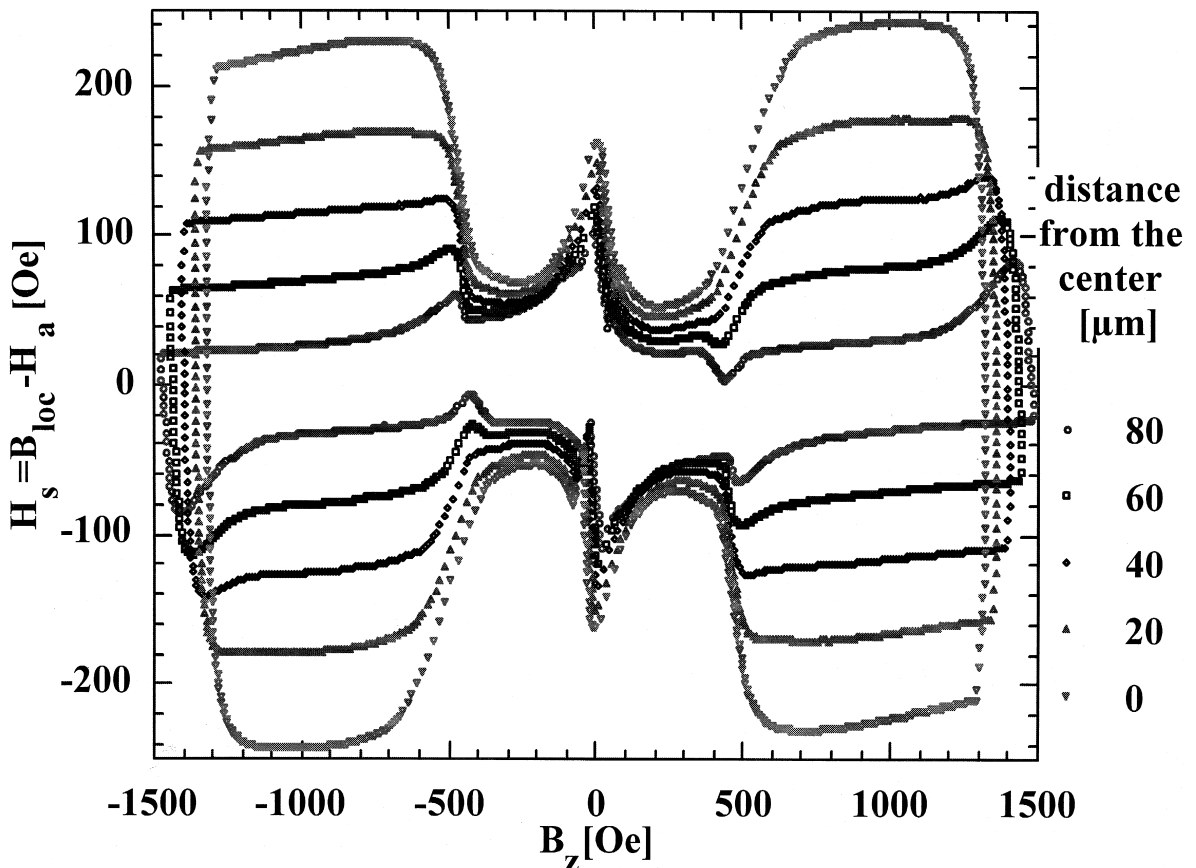


Fig. 1. Local magnetization loops recorded at 20 K on BSCCO crystal with ramp rate of 1.3 Oe/s. At $B_{sp} \approx 500$ G, an abrupt increase of the width of the hysteresis loop and the appearance of a field gradient in the bulk of the sample marks the crossover from a surface barrier-supported screening current to pinning in bulk.

was traced as function of the local induction for several probes inside the sample periphery. The Meissner state is marked by the vertical decrease of H_s , ($B_z = 0$) until the first flux penetration which, in the surface barrier regime, starts from the center of the sample. This regime, characterized by current flowing on the sample edge and a dome-shaped magnetic induction profile, persists up to applied fields of 500 Oe. At higher fields, sand-pile-like profiles of the magnetic induction develop, characteristic of a shielding current flowing in the bulk of the sample. This is easily visualized by the position dependence of the width of the local magnetization loop. The characteristic field B_{sp} at which the bulk shielding current emerges depends on the sample anisotropy that is controlled by its oxygen content [4]. We choose a slightly overdoped sample with an increased value of B_{sp} in order to enlarge the region of the phase diagram occupied by the low field vortex phase. Association of the low field part of the hysteresis loop with bulk pinning is a common misinterpretation of magnetization measurements of BSCCO. At temperatures above 20 K, the bulk current in clean crystals decays to values below the surface contribution on the time scale of a typical experiment ($t > 100$ s) [1,2]. As a consequence, the rise of the magnetization observed at the SP corresponds to the crossover from the surface barrier to the bulk pinning supported current. Hence, the direct comparison of energy barriers controlling flux creep below and above the SP, leading to a higher barrier (slower relaxation) in the low field phase, is meaningless. In order to access bulk pinning in the low field phase, we should either explore lower temperatures or use shorter times at which the bulk pinning current is sufficiently large. Since the acquisition of an induction profile from the Hall array takes at least 1 s, relaxation experiments are typically carried out in the interval 5–4000 s at temperatures slightly lower than 20 K.

At 14.8 K it is possible to observe magnetization loops similar to that presented in Fig. 1 by ramping extremely slowly, but at typical ramp rates above 0.1 Oe/s the crossover at the SP occurs between two regimes of bulk pinning. We then adopted the following procedure for recording the magnetic relaxation. The sample was cooled down from above 30 K in a field 3 kOe above the target field. When the

temperature was stabilized at 14.8 K, the external field was rapidly decreased (1 kOe/s) to the target value between 0 and 3 kOe, and the acquisition of magnetic induction profiles was started. A typical record of the decay of sand-pile-like induction profiles is shown in Fig. 2. In the case of target fields exceeding $B_{sp} \approx 500$ Oe, we observe a smooth decay of the local induction as well as that of the induction gradient $\partial B_z / \partial x$.

Following the approach of Abulafia et al. [12], we extract the creep energy barrier vs. current relation from the decay of the induction profiles. Using the Maxwell equation: $\partial B / \partial t = -\nabla \times E$ we convert the local $B_z(t)$ to the local electric field $E_y(x) = \int_0^x (\partial B_z / \partial t) dx'$. Assuming flux creep via thermally activated jumps over a current dependent energy barrier, the electric field due to flux motion reads: $E = Bv \propto B(\partial B / \partial x) \exp(-U/kT)$ and we obtain:

$$U(J) \propto -kT \ln \left(\int_0^x \frac{(\partial B_z / \partial t) dx'}{B(\partial B / \partial x)} \right). \quad (1)$$

The time derivatives $\partial B_z / \partial t$ are numerically calculated for each of Hall sensors, then the local electric field E is approximated by the sum of $\partial B_z / \partial t$ values from five sensors (from the center to the shaded area). The local gradient $\partial B_z / \partial x$ (which is proportional to the current density) and the average induction B_z are determined from B_z measured by the sensors placed 70–90 μm from the center. The obtained $U(J)$ relations are presented in Fig. 3. When the target field exceeds 500 Oe, a smooth increase of U with decreasing current was observed. Good approximations can be obtained either by power law function $U(J) \propto J^{-\mu}$, or by a logarithmic form. The value of $\mu \approx 0.3$ is too small to discern between a logarithmic and power law divergence of $U(J)$. It should be noted that during any relaxation process the local value of B_z varies simultaneously with the current. In result, the extracted value of U is in fact a function of both J and B . Since the curves recorded for several target fields between 500 and 800 Oe almost collapse onto one another, the B_z -dependence of the energy barrier can be neglected in comparison to the current dependence.

Drastically different results are obtained when the target field is below 500 Oe. First of all, the decay of

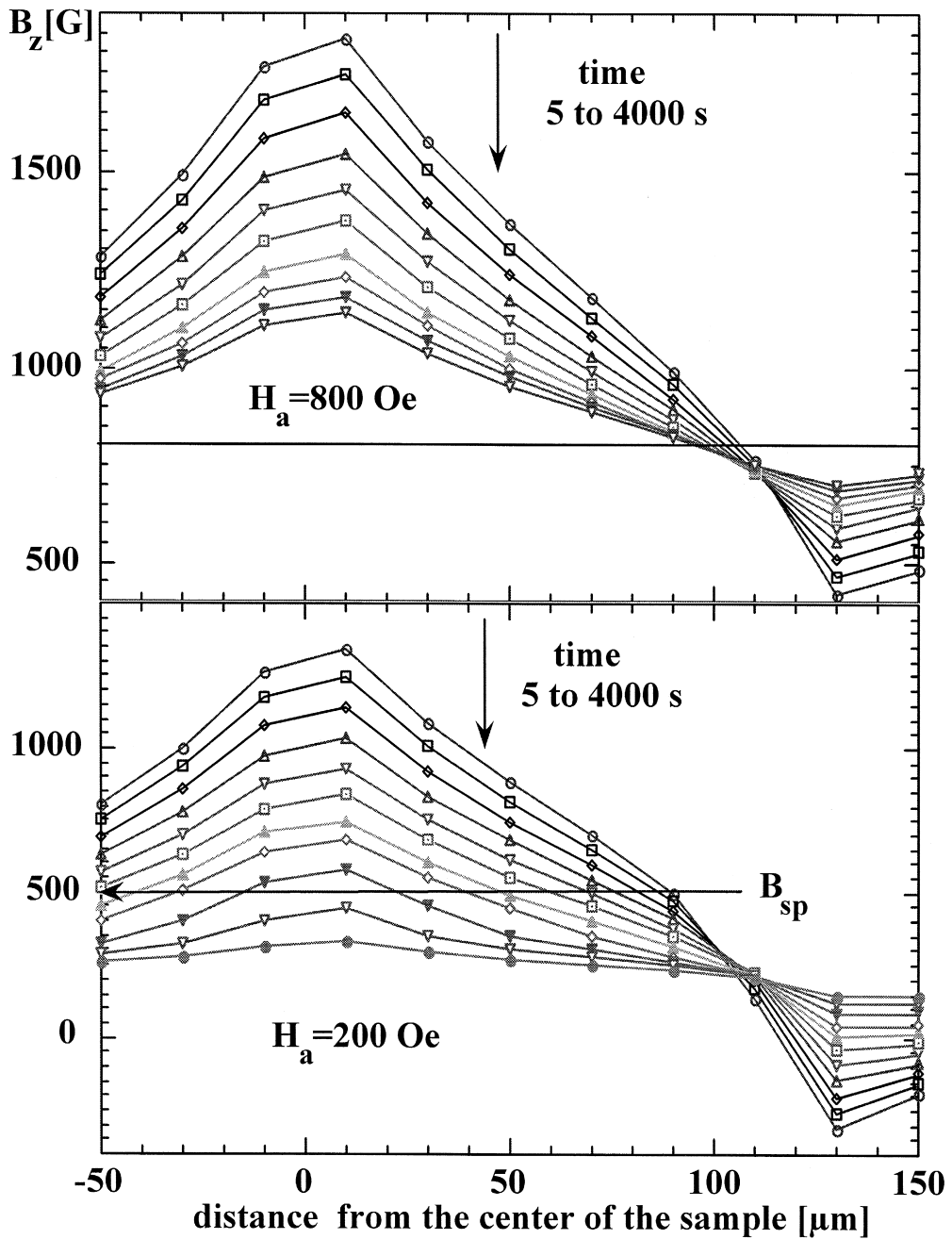


Fig. 2. Decay of the magnetic induction recorded by the Hall array placed on the surface of the BSCCO crystal, after field cooling from 30 to 14.8 K in a field 3 kOe higher than the target field, followed by rapid quenching of the field to 800 (upper panel) and 200 Oe (lower panel).

$\partial B_z / \partial x$ is not smooth anymore but exhibits a pronounced break at the point where the local magnetic

induction crosses $B_{sp} = 500 \text{ G}$. This can be seen on the lower panel of Fig. 2, showing decay of the

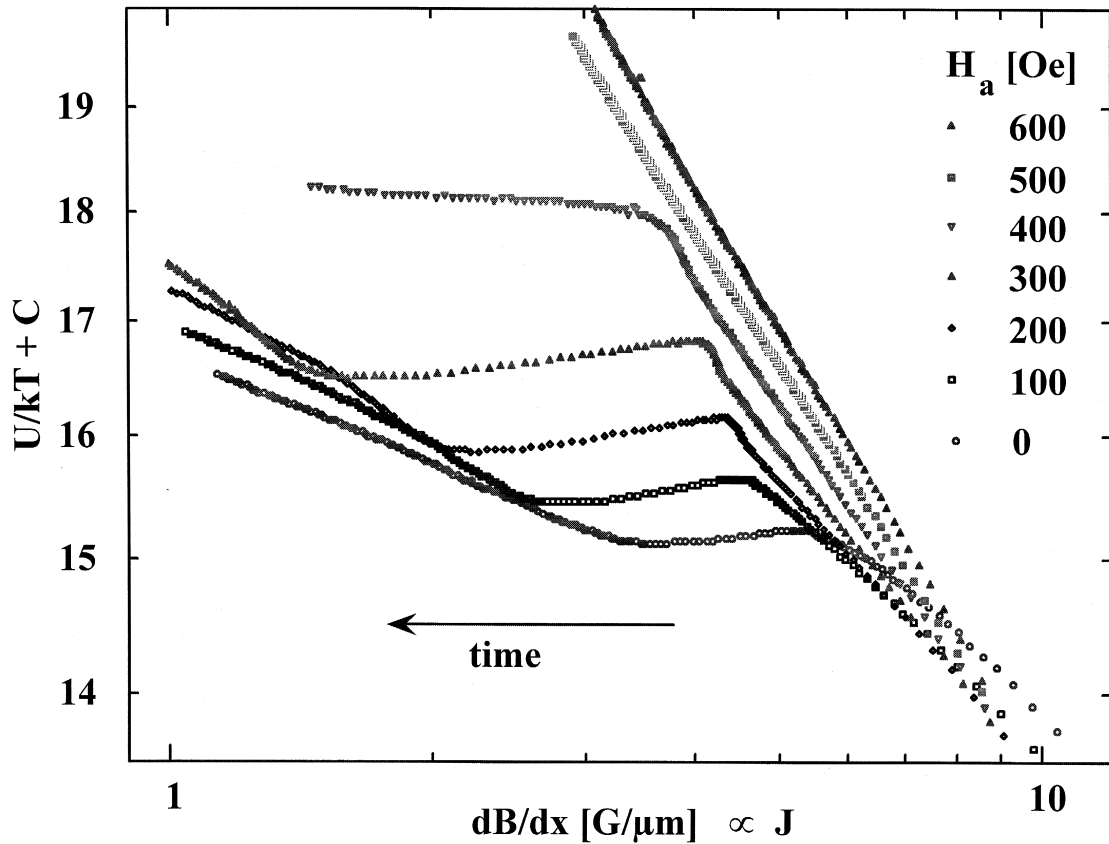


Fig. 3. Energy barrier for flux creep vs. current variation derived from flux exit relaxations recorded at 14.8 K on BSCCO crystal at various applied fields, following the procedure described in the text. A monotonic, power-law divergence of energy barrier ($U \propto J^{-0.3}$) is observed with decreasing current when the target field is larger than 500 Oe, corresponding to the onset of second peak in magnetization loop, B_{sp} . For lower target fields, an abrupt break on $U(J)$ curve appears at the point where the local magnetic field drops below B_{sp} , corresponding to the appearance of the low field vortex phase. When the magnetic induction drops below B_{sp} in the entire sample, a new, slower divergence shows up.

sand-pile profiles at a target field of 200 Oe. The energy barrier vs. current variation obtained in such a regime shows a more complicated feature: the divergence of U stops at the point where the local induction goes below B_{sp} value and remains flat until B_z falls below B_{sp} in the whole sample. At this point, the energy barrier starts to diverge again but following a much slower power law function. A good approximation of this low field part of the relaxation process is given by $U(J) \propto J^{-\mu}$, with $\mu \approx 0.1-0.08$. At 14.8 K, the magnetic induction profiles are always sand-pile-like even at the end of the relaxation process in contrast to higher temperatures when, under the same experimental conditions

the induction profiles converge to a dome-shape, and the surface barrier contribution cannot be neglected.

3. Discussion

The flux exit process in the BSCCO crystals at applied fields above B_{sp} is governed by the flux creep process in the high field glassy phase of the vortex lattice. From the analysis of the local magnetic relaxation, we obtained the $U(J)$ curve diverging as a power law at low J .

A completely novel situation arises when the applied magnetic field is dropped below B_{sp} after

preparation of a critical state above B_{sp} . The phase transformation takes place during the relaxation process and is measured by successive sensors as the phase transformation front propagates across the sample. This slow propagation of the phase boundary is responsible for the flat part of the apparent $U(J)$ curves shown in Fig. 3. In this regime, the description of relaxation as a unique flux creep process is inadequate. In the experiment presented in Figs. 2 and 3, the relaxation process in the low field phase is much faster than in the high field phase, which means that for a given current the energy barrier for flux creep is much higher in the latter. In the case concerned here, the slow propagation of the phase boundary determines the overall magnetic relaxation. The sole existence of the phase boundary is not sufficient to determine the order of the phase transition. On the background of magnetic irreversibility, a field gradient may lead to phase separation and a sharp phase boundary even in the case of a second order transition.

The energy barrier–current relation of the low field phase was inferred from the long time behavior of the decay, after the phase transformation has occurred in the whole sample. The divergence of the energy barrier with decreasing current is much slower in this phase; thus for the currents explored in our experiments, the actual value of the barrier for a given current is higher in the high field phase than in the low field phase. This does not mean that the critical current is higher in the disordered high field phase, the logarithmic extrapolation of obtained $U(J)$ curves to high current values lets us anticipate a crossing point and the inverse situation with a higher barrier in low field phase. This is indeed observed at much lower temperatures at which we accessed much higher currents.

In summary, we demonstrate that the phenomenology of the SP in clean BSCCO is a conjunction of three processes. The magnetic relaxation in

two distinct vortex phases is characterized by two $U(J)$ curves that diverge in the low current limit. However, the barrier divergence is much stronger in the high field phase with respect to that at low fields. Since in the relaxing system the shielding current is self-adjusted by the condition $U(J) \approx kT \ln(t)$ [13], the phase transition leads to an abrupt variation of shielding current. A novel process of slow propagation of the phase transformation front across the sample was found to contribute to the overall relaxation process in the vicinity of the SP.

References

- [1] N. Chikumoto, M. Konczykowski, N. Motohira, K. Kishio, K. Kitazawa, *Physica C* 185–189 (1991) 2201.
- [2] N. Chikumoto, M. Konczykowski, N. Motohira, A.P. Malozemoff, *Phys. Rev. Lett.* 69 (1992) 1260.
- [3] E. Zeldov, D. Majer, M. Konczykowski, V.B. Geshkenbein, V.M. Vinokur, H. Strikman, *Nature* 375 (1995) 373.
- [4] B. Khaykovich, E. Zeldov, D. Majer, T.W. Li, P.H. Kes, M. Konczykowski, *Phys. Rev. Lett.* 76 (1996) 2555.
- [5] B. Khaykovich, M. Konczykowski, E. Zeldov, R.A. Doyle, P.H. Kes, D. Majer, T.W. Li, *Phys. Rev. B* 56 (1997) R517.
- [6] D. Ertaş, D.R. Nelson, *Physica C* 272 (1996) 79.
- [7] T. Giamarchi, P. LeDoussal, *Phys. Rev. B* 55 (1997) 6577.
- [8] V.M. Vinokur, B. Khaykovich, E. Zeldov, M. Konczykowski, R.A. Doyle, P.H. Kes, *Physica C* 295 (1998) 209.
- [9] R. Cubitt, E.M. Forgan, G. Yang, S.L. Lee, D. McK. Paul, H.A. Mook, M. Yethiraj, P.H. Kes, T.W. Li, A.A. Menovsky, Z. Tarnawski, K. Mortensen, *Nature* 365 (1993) 410.
- [10] S.L. Lee, P. Zimmerman, H. Keller, M. Warden, I.M. Savic, R. Schauwecker, D. Zech, R. Cubitt, E. Forgan, P.H. Kes, T.W. Li, A.A. Menovsky, Z. Tarnawski, *Phys. Rev. Lett.* 71 (1993) 3862.
- [11] I. Joumard, J. Marcus, T. Klein, R. Cubitt, *Phys. Rev. Lett.* 82 (1999) 4930.
- [12] Y. Abulafia, A. Shaulov, Y. Wolfus, L. Burlachkov, Y. Yeshurun, D. Majer, E. Zeldov, V.M. Vinokur, *Phys. Rev. Lett.* 75 (1995) 2404.
- [13] V.B. Geshkenbein, A.I. Larkin, *Zh. Eksp. Teor. Fiz.* 95 (1989) 1108, (*Sov. Phys. JETP* 68 (3) (1989) 639).